Wind Energ. Sci. Discuss., doi:10.5194/wes-2016-54, 2016
Manuscript under review for journal Wind Energ. Sci.
Published: 20 December 2016

eawe european academy of wind energy
Open Access WIND ENERGY SCIENCE DISCUSSIONS

Simulation of an offshore wind farm using fluid power for centralized electricity generation

Antonio Jarquin Laguna

Section Offshore Engineering, Faculty of Civil Engineering and Geosciences, Delft University of Technology, Stevinweg 1, 2628 CN, Delft, The Netherlands

Correspondence to: A.JarquinLaguna@tudelft.nl

Abstract. A centralized approach for electricity generation within a wind farm is explored through the use of fluid power technology. This concept considers a new way of generation, collection and transmission of wind energy inside a wind farm, in which electrical conversion does not occur during any intermediate conversion step before the energy has reached the offshore central platform. A numerical model was developed to capture the relevant physics from the dynamic interaction between different turbines coupled to a common hydraulic network and controller. This paper presents two examples of the time-domain simulation results for a hypothetical hydraulic wind farm subject to turbulent wind conditions. The performance and operational parameters of individual turbines are compared with those of a reference wind farm with conventional technology turbines, using the same wind farm layout and environmental conditions. For the presented case study, results indicate that the individual wind turbines are able to operate within operational limits with the current pressure control concept. Despite the stochastic turbulent wind input and wake effects, the hydraulic wind farm is able to produce electricity with reasonable performance in both below and above rated conditions.

1 Introduction

A typical offshore wind farm consists of an array of individual wind turbines several kilometers from shore. Each of these turbines captures the kinetic energy from the wind and converts it into electrical power in a similar way as is done with onshore technology. However, one main characteristic of a wind farm as a collection of individual turbines, is that electricity is still generated in a distributed manner. This means that the whole process of electricity generation occurs separately and is then collected, conditioned and transmitted to shore. When looking at a wind farm as a power plant, it seems reasonable to consider the use of only a few generators of larger capacity rather than around one hundred of generators of lower capacity. The potential benefits, challenges and limitations of a centralized electricity generation scheme for an offshore wind farm are not known yet.

This work explores a particular concept in which a centralized electricity generation within a wind farm is proposed by means of a hydraulic network using fluid power technology (Diepeveen, 2013). The basic idea behind the concept is to dedicate the individual wind turbines to create a pressurized flow of seawater. Then, the flow is collected from the turbines and redirected through a network of pipelines to a central generator platform. At the platform, the overall pressurized flow is converted first

Wind Energ. Sci. Discuss., doi:10.5194/wes-2016-54, 2016
Manuscript under review for journal Wind Energ. Sci.
Published: 20 December 2016

into mechanical and later into electrical power through an impulse hydraulic turbine. A conceptual comparison between a conventional and the proposed offshore wind farm is shown in Fig. 1.

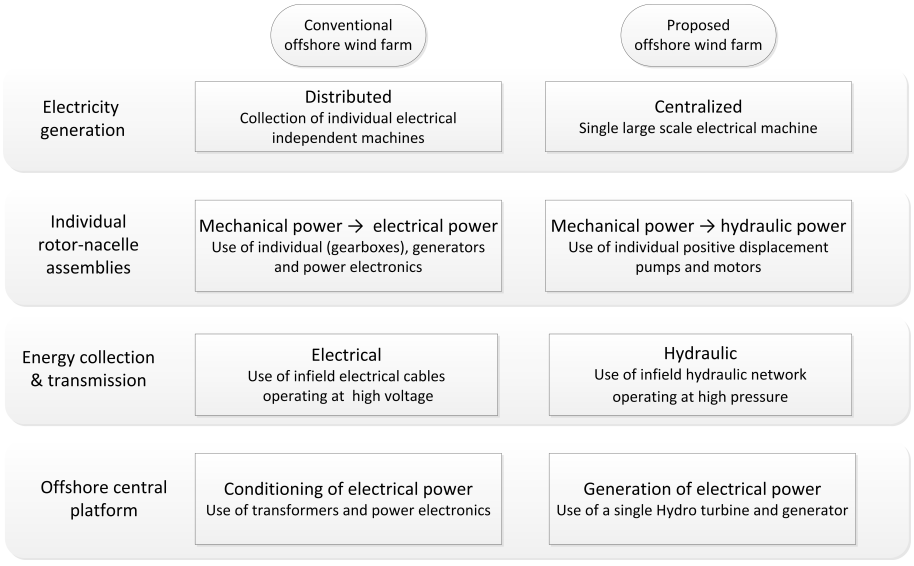

Figure 1. Conceptual comparison between a conventional and the proposed offshore wind farm.

This paper continues with previous work (Jarquin Laguna et al., 2014; Jarquin Laguna, 2015) in an effort to asses the trade-offs implied by the proposed hydraulic concept. To this aim, time domain simulations are used to evaluate the performance and operational parameters of individual turbines coupled to a common hydraulic network for a hypothetical wind farm with centralized electricity generation. In the first part of this work, an overview of the wind farm model is presented together with the control strategy of the hydraulic components; the second part describes a case example where the results are compared with those of a typical wind farm.

2 Wind farm model overview

The overall wind farm model, incorporates the dynamic interaction between the individual turbines, the hydraulic network, the Pelton turbine and the controller. The model is described as a set of coupled algebraic and non-linear ordinary differential equations which are solved by numeric integration using Matlab-Simulink. The hydraulic wind power plant model is composed by the following subsystems:

Wind Energ. Sci. Discuss., doi:10.5194/wes-2016-54, 2016
Manuscript under review for journal Wind Energ. Sci.
Published: 20 December 2016

eawe european academy of wind energy
Open Access WIND ENERGY SCIENCE DISCUSSIONS

2.1 Wind turbines

2.1.1 Aerodynamic model

The aerodynamic characteristics of a horizontal axis wind turbine rotor are a function of its rotational speed ω_r, the pitch angle of the blades β and the relative velocity of the upstream wind speed U with respect to the rotor. The torque τ_{aero}, and axial thrust F_{thrust} performance are described through their non-dimensional steady-state coefficients as a function of the upstream wind speed.

$$\tau_{aero} = C_\tau(\lambda,\beta)\,\frac{1}{2}\,\rho_{air}\,\pi\,R^3\,U_{rel}^2 \tag{1}$$

$$F_{thrust} = C_{Fax}(\lambda,\beta)\,\frac{1}{2}\,\rho_{air}\,\pi R^2\,U_{rel}^2 \tag{2}$$

$$\tag{3}$$

where ρ_{air} is the air density, R is rotor radius and the tip speed ratio λ is defined as the tangential velocity of the blade tip and the upstream undisturbed wind speed.

$$\lambda = \frac{\omega_r\,R}{U_{rel}} \tag{4}$$

This reduced order model does not include any aero-elastic or unsteady aerodynamic effects. Although these aspects are important for the loading of both rotor and support structure, their effects on the aerodynamic torque are considered less relevant from the performance and control point of view of the overall wind farm; the relatively large mass moment of inertia of the rotor in the angular degree of freedom, will absorb large peak fluctuations in the rotor speed derived from the unsteady aerodynamic effects on the rotor torque.

2.1.2 Hydraulic drive train model

The hydraulic drive train consists of a large positive displacement water pump directly coupled to the low-speed rotor shaft. Hence, the rotor-pump angular acceleration is described through the balance of the aerodynamic torque τ_{aero}, and the transmitted torque from the pump τ_p as a first order differential equation; the mass moment of inertia of the rotor and pump is described by:

$$J_r\,\dot{\omega}_r - \tau_{aero}\,(U,\beta,\omega_r) + \tau_p\,(\omega_r,\Delta p_p,V_p) = 0 \tag{5}$$

The pump is mainly characterized through a variable volumetric displacement V_p, which determines the volume of fluid that is obtained per rotational displacement. Hence the volumetric flow rate of the pump Q_p is ideally given by the product of its volumetric displacement and the rotor shaft speed; internal leakage losses are included as a linear function of the pressure drop

Wind Energ. Sci. Discuss., doi:10.5194/wes-2016-54, 2016
Manuscript under review for journal Wind Energ. Sci.
Published: 20 December 2016

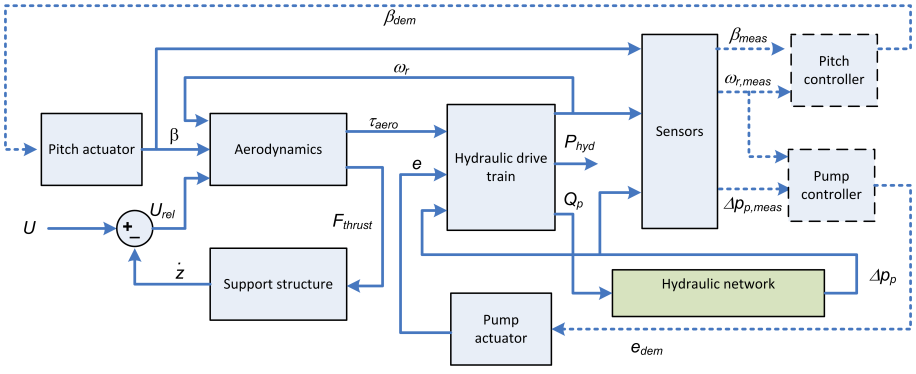

Figure 2. Subsystem block diagram a of a single turbine connected to the hydraulic network.

across the pump Δp with the laminar leakage coefficient C_s. In a similar manner, the transmitted torque is directly related to the volumetric displacement and the pressure across the pump; a friction torque is described with a viscous and a dry component defined with the damping coefficient B_p and a friction coefficient C_f respectively (Merritt, 1967).

$$Q_p = V_p(e)\,\omega_r - C_s\,\Delta p_p \tag{6}$$

$$\tau_p = V_p(e)\,\Delta p_p + B_p\,\omega_r + C_f\,V_p(e)\,\Delta p_p \tag{7}$$

here e is introduced as the ratio of the current volumetric displacement and its nominal value per rotational cycle such that:

$$V_p = e\,V_{p,max} \tag{8}$$

the variable e from Eq. (8) is used as a control variable to modify either the volumetric flow rate or the transmitted torque of the pump. The dynamics of a general actuator used to modify the volumetric displacement of the pump, are approximated by a first order differential equation. The constant T_e characterizes how slow or fast the actuator responds to a reference value input e_{dem} according to the following equation:

$$\dot{e} = \frac{1}{T_e}\,(e_{dem} - e) \tag{9}$$

The yaw degree of freedom of the individual turbines is not considered. Hence, the yaw controller of the turbines is not included. A schematic showing the different subsystems of a single turbine is shown in Fig. 2.

2.1.3 Pitch actuator model

The pitch actuator is based on a pitch-servo model described by a proportional regulator with constant K_β. The demanded pitch β_{dem} is obtained from the signal of the pitch controller. The second order model includes a time constant t_β and an input

Wind Energ. Sci. Discuss., doi:10.5194/wes-2016-54, 2016
Manuscript under review for journal Wind Energ. Sci.
Published: 20 December 2016

eawe european academy of wind energy
Open Access WIND ENERGY SCIENCE DISCUSSIONS

delay δ from input u_β to the pitch rate $\dot{\beta}$; the delayed input is expressed as u_β^δ. The pitch actuator is implemented with pitch rate limits of $\pm 8°$.

$$\ddot{\beta} = \frac{1}{t_\beta}\left(u_\beta^\delta - \dot{\beta}\right) \tag{10}$$

$$u_\beta = K_\beta\left(\beta_{dem} - \beta_{meas}\right) \tag{11}$$

2.1.4 Structural model

The motion of the top mass of the tower in the fore-aft direction z is described with a second order model:

$$m_{tm}\,\ddot{z} = F_{thrust} - B_{tower}\,\dot{z} - K_{tower}\,z \tag{12}$$

where K_{tower} and B_{tower} are the support structure stiffness and damping; F_{thrust} is the thrust force exerted by the rotor on the top mass of the tower m_{tm}, which includes the rotor and nacelle mass.

2.2 Hydraulic network

One of the key aspects for having a centralized electricity generation is the use of hydraulic networks to collect and transport the pressurized water from the individual wind turbines to the generator platform. Similarly to the electrical inter-array cable system for a conventional offshore wind farm, the design of the hydraulic lay-out should consider several practical and economical aspects, such as reducing the number and length of pipelines, operational losses and installation methods. For wind farms with a large number of turbines, it is expected that branched hydraulic networks using parallel and common pipelines will result in the most convenient configuration. The hydraulic network consists of a number of interconnected pipelines represented by linear transmission line models. The approach to construct this networks for time-domain simulations from individual pipelines was previously presented in (Jarquin Laguna et al., 2014). The dynamic response of the compressible laminar flow of a Newtonian fluid through a rigid pipeline network is given by the following state-space model; the model includes inertia and compressibility effects which are necessary to describe the fluid transients or so-called 'water-hammer' effects. The model uses the volumetric flow rates from the individual rotor driven pumps and at the nozzle as an input, and the pressures at across the water pumps and nozzle as an output.

$$\text{Hydraulic network model} \begin{cases} \dot{\mathbf{x}} = \mathbf{A_Q}\mathbf{x} + \mathbf{B_Q}\begin{pmatrix} Q_{p,1} \\ Q_{p,2} \\ \vdots \\ Q_{p,i} \\ Q_{nz} \end{pmatrix}, & \begin{pmatrix} \Delta p_{p,1} \\ \Delta p_{p,2} \\ \vdots \\ \Delta p_{p,i} \\ \Delta p_{nz} \end{pmatrix} = \mathbf{C_Q}\mathbf{x} \end{cases} \tag{13}$$

Wind Energ. Sci. Discuss., doi:10.5194/wes-2016-54, 2016
Manuscript under review for journal Wind Energ. Sci.
Published: 20 December 2016

eawe european academy of wind energy
Open Access WIND ENERGY SCIENCE DISCUSSIONS

The matrices $\mathbf{A_Q}$, $\mathbf{B_Q}$ and $\mathbf{C_Q}$ are defined in terms of the physical parameters of the hydraulic lines and water properties such as water viscosity, water density, speed of sound in the water, length and internal radius of the pipelines. A schematic of the model showing the input-output causality for each element is shown in Fig. 3.

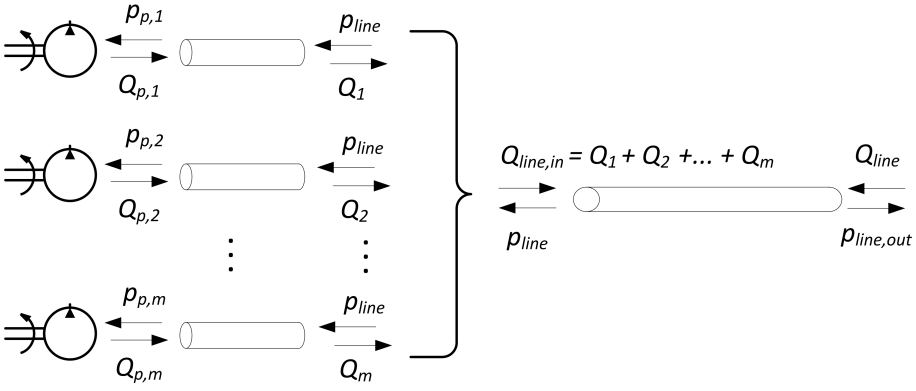

Figure 3. Schematic for parallel hydraulic lines connected to a common line.

2.3 Nozzle and spear valve

At the end of the hydraulic network, a nozzle and spear valve is used to adapt the pressurized water flow into the Pelton turbine. The nozzle characteristics are included as a first order differential equation by taking the momentum equation of a fluid particle into account along the nozzle length L_{nz} as described in Eq. (14), (Makinen et al., 2010).

$$\rho_{hyd}\, L_{nz}\, \dot{Q}_{nz} = \Delta p_{nz}\, A_{nz}\,(h_s) - \frac{\rho_{hyd} Q_{nz} |Q_{nz}|}{2 A_{nz}\,(h_s)\, C_d^2} \tag{14}$$

Where ρ_{hyd} is the density of the hydraulic fluid, A_{nz} is the nozzle cross sectional area determined by the position of the spear valve, and C_d is the discharge coefficient to account for pressure losses due to the geometry and flow regime at the nozzle exit. The nozzle cross sectional area is described by the linear position of the spear valve h_s according to Eq. (15). It is assumed that the spear valve position is smaller than the fixed nozzle diameter d_s. The geometric characteristics of the spear valve are included through the spear cone angle α as shown in Figure 4.

$$A_{nz}\,(h_s) = min\left(\pi \left[h_s\, d_s \sin\left(\frac{\alpha}{2}\right) - h_s^2 \sin^2\left(\frac{\alpha}{2}\right) \cos\left(\frac{\alpha}{2}\right)\right], \frac{\pi}{4} d_s^2\right)) \tag{15}$$

Figure 5 shows the normalized cross sectional area of the nozzle as function of the spear valve linear position for different spear cone angles.

Wind Energ. Sci. Discuss., doi:10.5194/wes-2016-54, 2016
Manuscript under review for journal Wind Energ. Sci.
Published: 20 December 2016

eawe european academy of wind energy
Open Access WIND ENERGY SCIENCE DISCUSSIONS

Similarly to the pump actuator, the dynamics of the spear valve linear actuator are approximated by a first order differential equation in which a constant T_h characterizes how slow or fast the spear valve position responds to reference value input $h_{s,dem}$ according to the following equation:

$$\dot{h}_s = \frac{1}{T_h}\left(h_{s,dem} - h_s\right) \tag{16}$$

The hydraulic power at the nozzle P_{hyd} is given by the product of the volumetric flow rate and the water pressure at this location.

$$P_{hyd} = Q_{nz}\,\Delta p_{nz} \tag{17}$$

2.4 Pelton turbine

The hydraulic efficiency of the Pelton runner η_P is obtained from momentum theory according to different geometrical and operational parameters as described in (Thake, 2000) and (Zhang, 2007).

$$\eta_P = 2k\left(1-k\right)\left(1-\xi\cos\gamma\right) \tag{18}$$

where ξ is an efficiency factor to account for the friction of the flow in the bucket, γ is defined as the angle between the circumferential and relative velocities, and k is the runner speed ratio defined by the ratio between the tangential velocity of the runner at Pitch Circle Diameter (PCD) and the jet speed.

$$k = \frac{\omega_P R_{PCD}}{U_{jet}} \tag{19}$$

For this case, the Pelton rotational speed is fixed to the synchronous speed of the generator. Thus, the efficiency of the Pelton turbine is only determined by the water jet velocity U_{jet}, which is simply the volumetric flow rate divided by the cross sectional

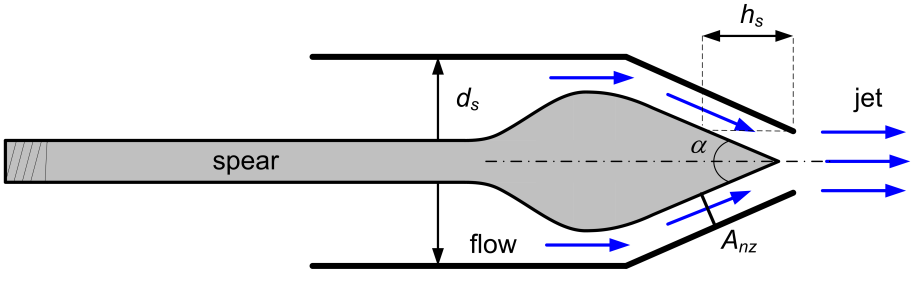

Figure 4. Schematic of the spear valve and nozzle.

Wind Energ. Sci. Discuss., doi:10.5194/wes-2016-54, 2016
Manuscript under review for journal Wind Energ. Sci.
Published: 20 December 2016

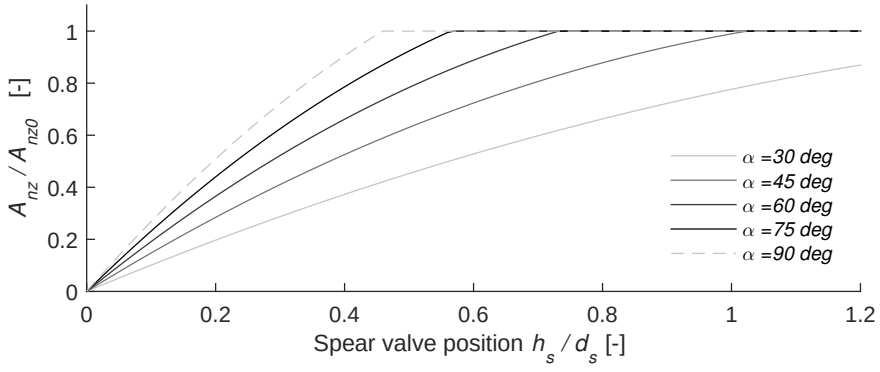

Figure 5. Cross sectional area of the nozzle as function of the spear valve linear position for different spear cone angles where $A_{nz0} = \frac{\pi}{4} d_s^2$.

area and multiplied by a vena contracta coefficient C_v to account for the change in velocity immediately after the water jet exits the nozzle.

$$U_{jet} = C_v \frac{Q_{nz}}{A_{nz}(h_s)} \tag{20}$$

2.5 Environmental conditions

The dynamic wind flow models and wake effects for a given layout are based on an open source toolbox developed for 'Distributed Control of Large-Scale Offshore Wind Farms' as part of the European FP7 project with the acronym Aeolus (Grunnet et al., 2010). The model assumes a 2D wind field generated at the hub height plane. The wind field does not account for wind shear or tower shadow effects and is generated at hub height plane. The mean wind speed has a constant value in the longitudinal direction and zero lateral component. Similarly, the wind speed direction is fixed with respect to the farm layout in longitudinal direction. The turbulent wind field is generated using a Kaimal spectrum; two spectral matrices together with coherence parameters are used to describe the spatial variations of the wind speed according to (Veers, 1988).

Three wake effects are considered: deficit, expansion and center, where wake deficit is a measure of the decrease in downwind wind speed, wake expansion describes the size of the downwind area affected by the wake and wake center defines the lateral position (meandering) of the wake area. Expressions for wake deficit, center and expansion were developed in (Frandsen et al., 2006; Jensen, 1983). To illustrate this, a small wind farm comprising of five turbines is shown in the layout of Fig. 6. Figure 7 shows a snapshot of the wind field where the wake effects are observed.

Wind Energ. Sci. Discuss., doi:10.5194/wes-2016-54, 2016
Manuscript under review for journal Wind Energ. Sci.
Published: 20 December 2016

eawe european academy of wind energy
Open Access WIND ENERGY SCIENCE DISCUSSIONS

3 Variable speed control strategy

The so called variable-speed operation is of particular interest for this concept because by removing the individual generators and power electronics from the turbines, the hydraulic drives need to replace the control actions to obtain the variable-speed functionality.

3.1 Pump controller

As shown in Eq. (7), it is possible to manipulate the transmitted torque of the pump using two different control degrees of freedom (in contrast with the electro-magnetic torque in a conventional turbine): the volumetric displacement of the pump and/or the pressure across it. In this case, the volumetric displacement of the pump from each turbine is controlled under a relatively constant pressure supply. Hence, the rotational speed of each rotor is able to be modified independently according to the local wind speed conditions. This strategy is commonly known in hydraulic systems as 'secondary control' (Murrenhoff, 1999). The required volumetric displacement of the pump e_{dem} is shown in Eq. (21) as a function of the measured rotational speed of the rotor $\omega_{r,meas}$ and the measured pressure at the pump location $\Delta p_{p,meas}$. A low pass filter on the pressure measurement is employed to prevent actuation from the fluid transient fluctuations in the hydraulic network. The reference torque τ_{ref} is obtained from the steady-state torque-speed curves defined for different operating regions as in conventional variable-speed control strategies.

$$e_{dem} = \frac{\tau_{ref}\left(\omega_{r,meas}\right) - B_p \omega_{r,meas}}{V_p\left(1 + C_f\right)\Delta p_{p,meas}} \tag{21}$$

3.2 Spear valve controller

In order to achieve a constant pressure in the hydraulic network, the linear actuation of the spear valve is used to constrict or release the flow rate through the nozzle area. The pressure control is based on a PI feedback controller and a cascade

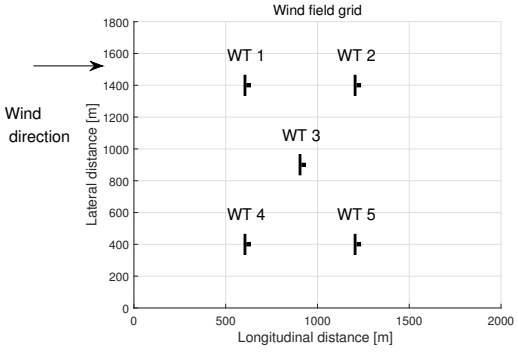

Figure 6. Layout of the proposed wind farm with five turbines of 5MW each.

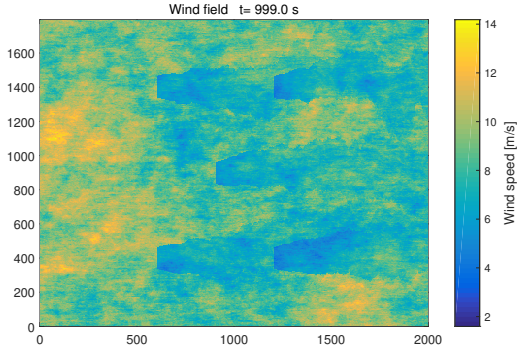

Figure 7. Snap shot of the wind field and wake effects.

Wind Energ. Sci. Discuss., doi:10.5194/wes-2016-54, 2016
Manuscript under review for journal Wind Energ. Sci.
Published: 20 December 2016

eawe european academy of wind energy
Open Access WIND ENERGY SCIENCE DISCUSSIONS

controller compensation to modify the linear position of the spear valve. A similar pressure control loop has been proposed in (Buhagiar et al., 2016); a schematic of the proposed controller is shown in Fig. 8.

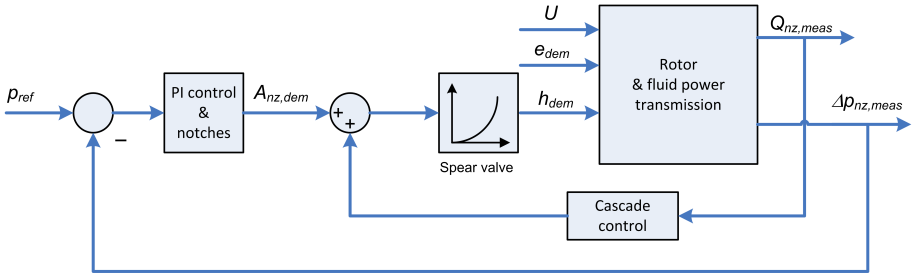

Figure 8. Pressure control schematic based on the spear valve position of the nozzle.

In order to prevent excitation from the low damped modes of the hydraulic network, the PI controller is augmented with a second order low pass filter and a series of notch filters. A schematic showing the structure of the augmented controller is shown in Fig. 9.

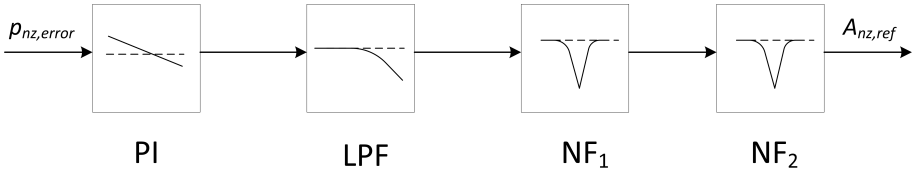

Figure 9. Schematic overview of the structure of the controller. The control blocks from left to right: Proportional-integral (PI), low-pass filter (LPF), notch filter 1 (NF1), notch filter 2 (NF2).

The low pass filter and the notch filters are described in the frequency domain according to Eqs. 22 and 23. The negative values of the proportional and integral gain show that if the reference pressure is higher than the measured pressure at the nozzle (positive error input to the controller), the controller action should reduce the nozzle area to constrict the flow rate and induce a higher pressure. This inverse relation is reflected in the negative values of the controller gains.

$$LPF(s) = \frac{\omega_{LPF}^2}{s^2 + 2\omega_{LPF}\,\zeta_{LPF} s + \omega_{LPF}^2} \tag{22}$$

$$NF_i(s) = \frac{s^2 + 2\omega_{ni}\,\zeta_{ni} s + \omega_{ni}^2}{s^2 + 2\omega_{ni}\,\beta_{ni} s + \omega_{ni}^2} \tag{23}$$

3.3 Pitch control

Above rated wind speed, the rated rotor speed is maintained by pitching collectively the rotor blades. A conventional PI pitch controller is proposed using the rotor speed error instead of the generator speed error. Due to the sensitivity of the aerodynamic

Wind Energ. Sci. Discuss., doi:10.5194/wes-2016-54, 2016
Manuscript under review for journal Wind Energ. Sci.
Published: 20 December 2016

eawe european academy of wind energy
Open Access WIND ENERGY SCIENCE DISCUSSIONS

response of the rotor to the pitch angle, the value of the controller gains are modified as a function of the pitch angle through a gain-scheduled approach. The gain scheduled PI controller is shown in the next equations, where $K_{P/I}$ are the proportional and integral gains respectively, $K_{P/I,0}$ is the gain at rated pitch angle $\beta = 0$, and β_K is the blade pitch angle at which the pitch sensitivity of aerodynamic power to rotor collective blade pitch has doubled from its value at the rated operating point.

$$\beta_{dem} = K_P(\beta)\,\omega_{r,error} + K_I(\beta)\int_0^t \omega_{r,error}\,dt \tag{24}$$

$$K_{P/I}(\beta) = K_{P/I,0}\,\frac{\beta_K}{\beta_K + \beta} \tag{25}$$

$$\omega_{r,error} = \omega_{r,rated} - \omega_{r,meas} \tag{26}$$

The values of the different gains are obtained in a similar way as described in (Jonkman et al., 2009), taking into account a modified apparent inertia at the low speed shaft and a transmission ratio which is set to one. To get rid of high frequency excitation, a low pass filter on the rotor speed measurement is used to prevent high frequency pitch action.

4 Simulation example

4.1 Wind farm conditions

The model described in the previous sections is used to assess the performance and operating conditions of a small hydraulic wind farm under specific wind conditions. Five turbines of $5\mathrm{MW}$ each are interconnected, through a hydraulic network, to a $25\mathrm{MW}$ Pelton turbine located at an offshore platform within $1\ \mathrm{km}$ distance from the individual turbines. Two different wind speeds corresponding to below and above rated conditions are simulated. First, a wind field with a mean wind speed of $9\ \mathrm{m/s}$ and 10% turbulence intensity (TI) is used as an input during $1000s$. For above rated conditions, a mean wind speed of $15\ \mathrm{m/s}$ and 12% TI is employed. The main parameters are shown in Table 1.

Table 1. Main design parameters for the offshore wind turbine with fluid power transmission.

Design parameter		Design parameter	
Rotor diameter	126 m	Drivetrain concept	Hydraulic
Rated wind speed	11.4 m/s	Nominal water pressure	150 bar
Design tip speed ratio λ	7.55	Pump volumetric disp	10.2 L/rpm
Max power coefficient C_P	0.485	Lines length	1 km
Rated power	5 MW	Lines diameter	0.5 m
Max blade tip speed	80 m/s	Nozzle nom diameter	43.2 mm

Wind Energ. Sci. Discuss., doi:10.5194/wes-2016-54, 2016
Manuscript under review for journal Wind Energ. Sci.
Published: 20 December 2016

The results from the simulations are compared with those of a reference wind farm comprising of 5MW NREL turbines (Jonkman et al., 2009), using the same wind farm layout and environmental conditions. A schematic of the individual turbines and configurations used in the simulation example for both wind farms is shown in Fig. 10. The capital letters A, B and C are used as a reference to present the results at specific points.

4.2 Time-domain results

The results of the time domain simulations are presented in terms of the main operational parameters such as mechanical power, rotor speed and pitch angle for the five turbines. For below rated conditions Fig. 11 shows the transient response of the reference and the hydraulic wind farm. The results demonstrate that for the considered scenario and with the current control strategy, the hydraulic wind farm is able to generate electricity from the pressurized water flow to the central platform via a Pelton turbine. In terms of performance it is observed that the turbines in the hydraulic wind farm experience higher excursions of the rotor speed in comparison with the reference case; this effect is also reflected in the increased pitch action required for the same wind speed conditions. A possible explanation of the more pronounced changes of the rotor speed is that the resulting torque demand generated by the hydraulic system is slower than in the reference case due to the higher fluid inertia of the hydraulic network. From a reliability point of view, the increased pitch action might have an important consequence on the life time of the pitch system. During the first 100s, the hydraulic wind farm shows high frequency fluctuations in the pressure and, consequently, in the total power output of the array. These higher fluctuations are due to the initial conditions of the pressure control settings in combination with the high fluid inertia in the hydraulic network. The changes in pressure and volumetric flow rate at the nozzle, have small influence on the efficiency of the Pelton turbine, which is maintained relatively constant and well above 90% during the whole simulation time, except for the first 100s of transient conditions.

For above rated conditions, the simulation results are shown in Fig. 12. It is observed that both concepts are able to keep the rotor speed operating within a constant speed band while producing relatively constant power. Likewise, the pitch actuation is very similar in both wind farms, which is not unexpected since the same pitch controller is used. Once more, the transient operation in the electrical power production is more pronounced in the case of the hydraulic wind farm because of the high hydraulic inertia of the hydraulic network. High frequency oscillations are observed in the electrical power as a consequence of the pressure waves travelling along the network.

Wind Energ. Sci. Discuss., doi:10.5194/wes-2016-54, 2016
Manuscript under review for journal Wind Energ. Sci.
Published: 20 December 2016

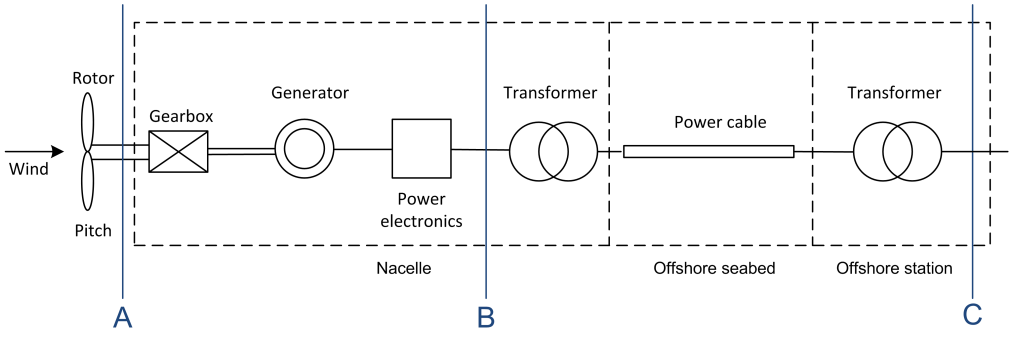

(a) NREL reference turbine.

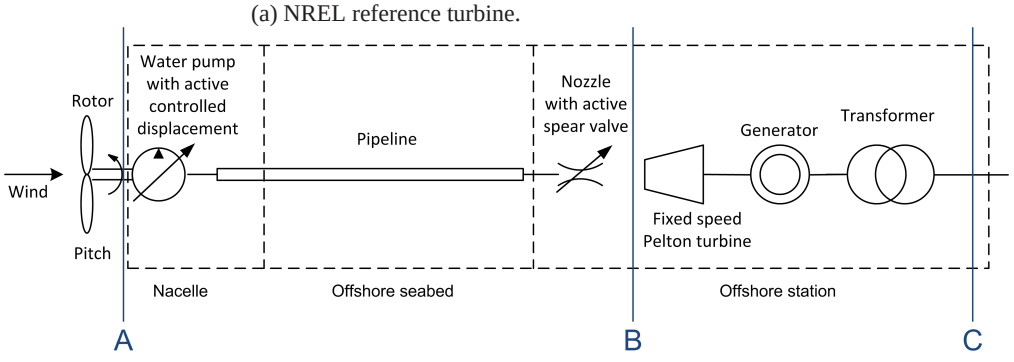

(b) Hydraulic turbine.

Figure 10. Simplified schematic with the main components involving the energy conversion for a reference offshore wind turbine and the proposed hydraulic concept.

Wind Energ. Sci. Discuss., doi:10.5194/wes-2016-54, 2016
Manuscript under review for journal Wind Energ. Sci.
Published: 20 December 2016

eawe european academy of wind energy
Open Access WIND ENERGY SCIENCE DISCUSSIONS

Table 2. Performance overview of time domain results for below rated conditions.

	Averaged power [MW]						Efficiency [-]		
	Mechanical		Transmitted		Electrical		Power coeff	A to B	B to C
Wind farm concept	point A		point B		point C		C_P	η_{AB}	η_{BC}
NREL reference	mean	std	mean	std	mean	std	mean	mean	mean
WT1	3.12	0.86	2.95	0.81	2.61	0.72	0.483	0.944	0.885
WT2	2.23	0.60	2.11	0.57	1.87	0.50	0.483	0.944	0.885
WT3	2.90	0.88	2.74	0.83	2.42	0.73	0.483	0.944	0.885
WT4	2.99	0.83	2.82	0.78	2.50	0.69	0.483	0.944	0.885
WT5	2.10	0.58	1.98	0.54	1.75	0.48	0.483	0.944	0.885
Total	13.3		12.6		11.1	1.90	-	-	-
Hydraulic with pressure control									
WT1	3.06	0.92	-	-	-	-	0.479	-	-
WT2	2.22	0.69	-	-	-	-	0.482	-	-
WT3	2.84	0.90	-	-	-	-	0.479	-	-
WT4	2.94	0.89	-	-	-	-	0.480	-	-
WT5	2.08	0.65	-	-	-	-	0.482	-	-
Total	13.1		11.6	2.58	10.2	2.71	-	0.88	0.877

Wind Energ. Sci. Discuss., doi:10.5194/wes-2016-54, 2016
Manuscript under review for journal Wind Energ. Sci.
Published: 20 December 2016

eawe european academy of wind energy
Open Access WIND ENERGY SCIENCE DISCUSSIONS

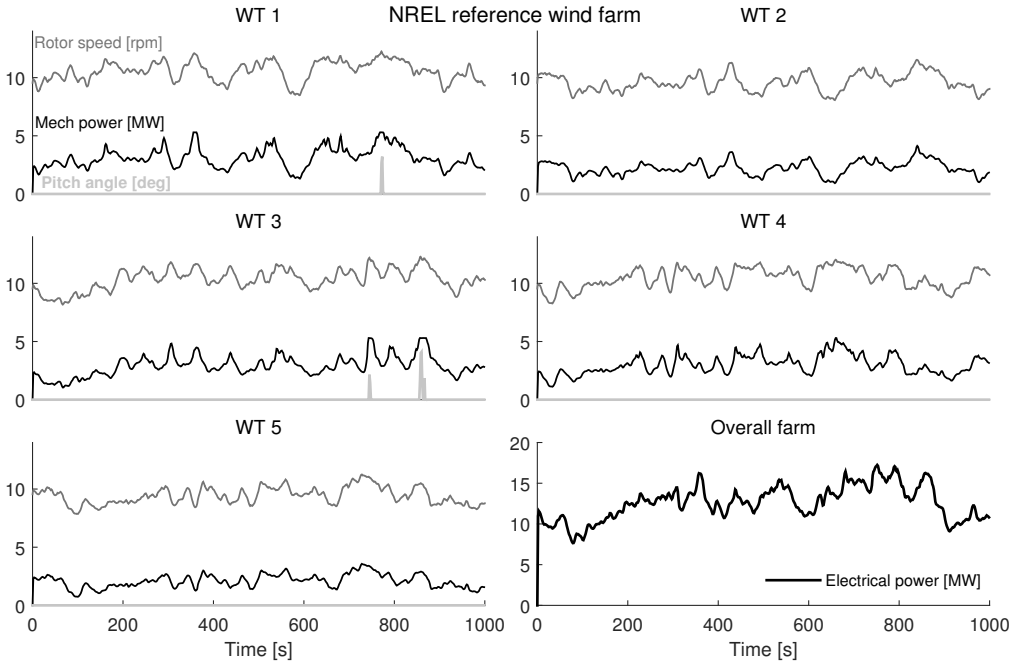

(a) Reference wind farm, below rated conditions.

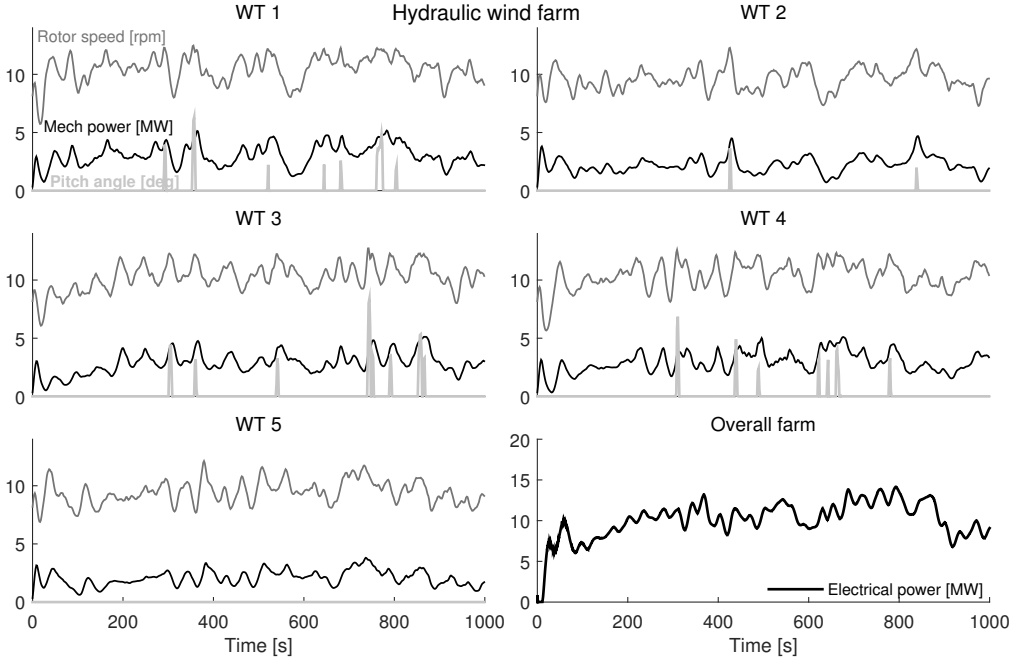

(b) Hydraulic wind farm, below rated conditions.

Figure 11. Time domain results for a wind farm comprising of 5 turbines subject to a wind field with a mean speed of 9 $\mathrm{m/s}$ and 10% turbulence intensity.

Wind Energ. Sci. Discuss., doi:10.5194/wes-2016-54, 2016
Manuscript under review for journal Wind Energ. Sci.
Published: 20 December 2016

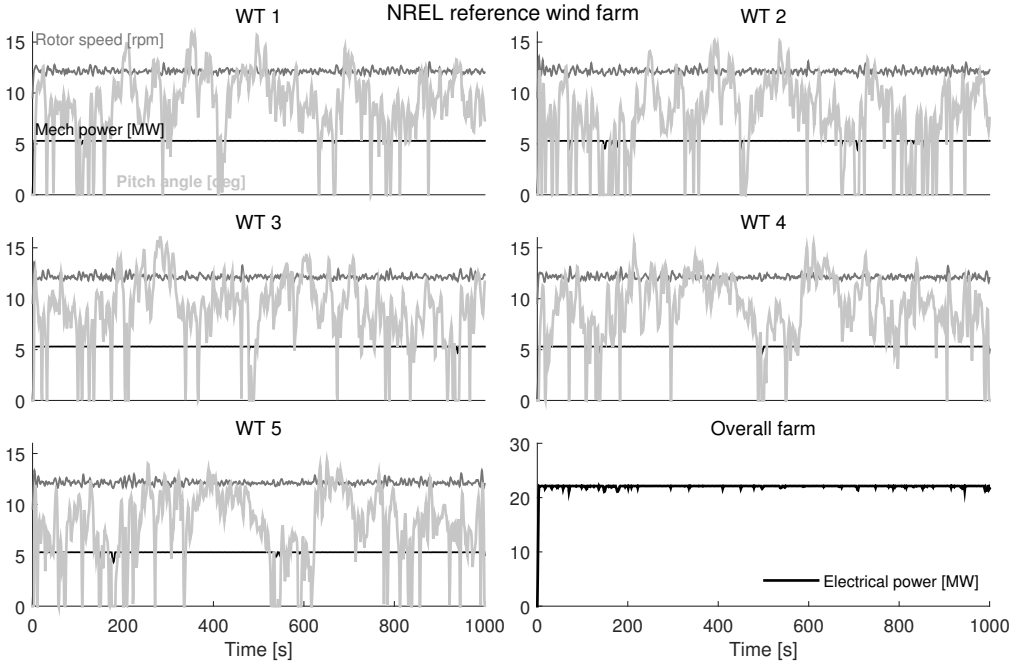

(a) Reference wind farm, above rated conditions.

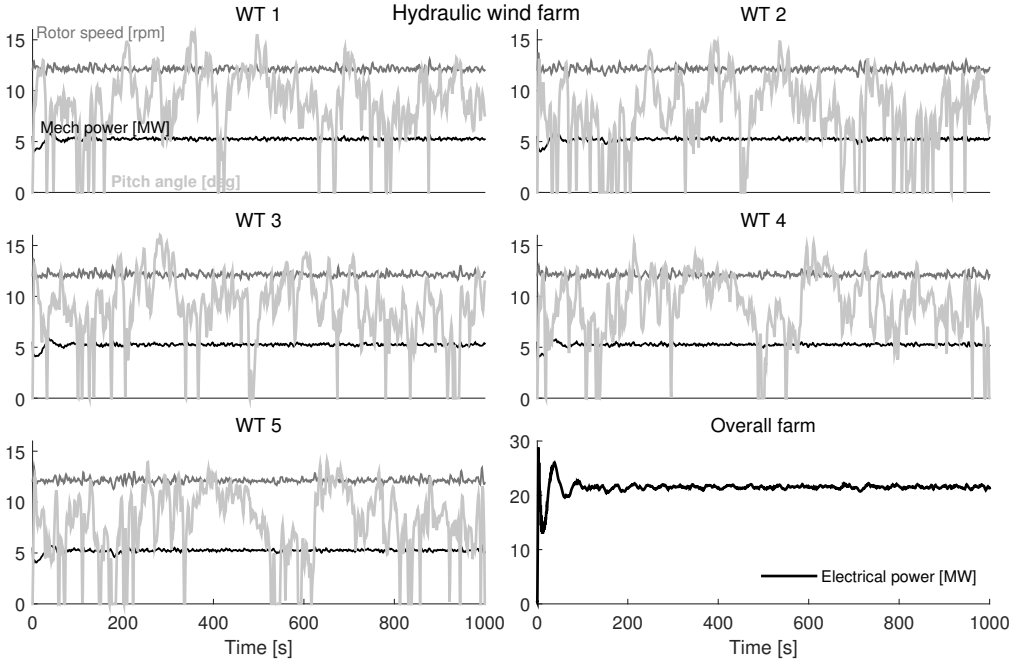

(b) Hydraulic wind farm, above rated conditions.

Figure 12. Time domain results for a wind farm comprising of 5 turbines subject to a wind field with a mean speed of 15 $\mathrm{m/s}$ and 12% turbulence intensity.

Wind Energ. Sci. Discuss., doi:10.5194/wes-2016-54, 2016
Manuscript under review for journal Wind Energ. Sci.
Published: 20 December 2016

eawe european academy of wind energy
Open Access WIND ENERGY SCIENCE DISCUSSIONS

4.3 Performance comparison

The performance of both wind farms for the considered conditions is summarized in the bar charts of Figs. 13 and 14 where the averaged values with the standard deviation of the power transmission and conversion are displayed. The numerical values together with the averaged efficiencies are summarized in Tables 2 and 3.

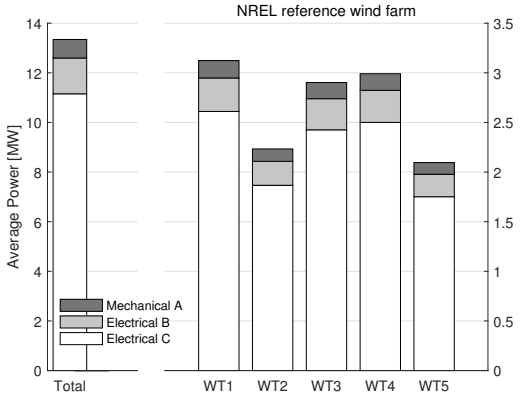

Figure 13. Power performance for the reference wind farm, below rated conditions.

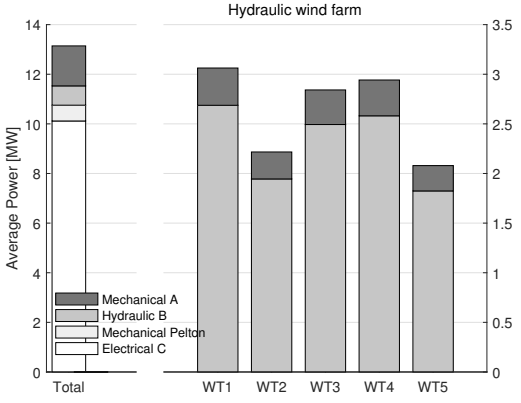

Figure 14. Power performance for the hydraulic wind farm, below rated condition.

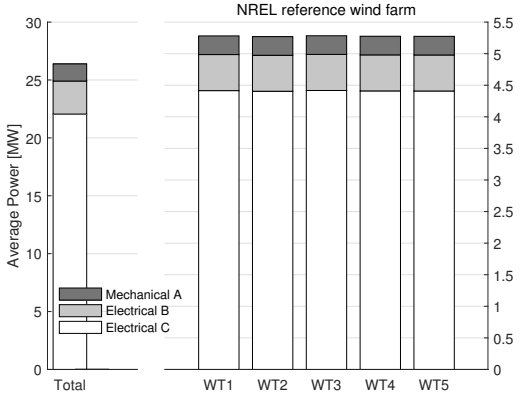

Figure 15. Power performance for the reference wind farm, above rated conditions.

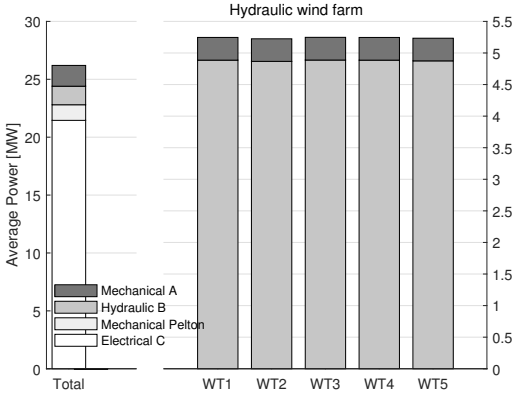

Figure 16. Power performance for the hydraulic wind farm, above rated conditions.

The first observation based on the general results for both wind farms is the reduced power performance of turbines WT2 and WT5. The performance of these two turbines is directly affected by the generated wake from turbines WT1 and WT4. In contrast, turbines WT1, WT3 and WT4 are not affected by any other wake interaction.

After including the performances of the main subsystems involved in the conversion and transmission of wind energy in a wind farm, the results show that the overall efficiency of a hydraulic wind farm is lower for a hydraulic concept compared

Wind Energ. Sci. Discuss., doi:10.5194/wes-2016-54, 2016
Manuscript under review for journal Wind Energ. Sci.
Published: 20 December 2016

eawe european academy of wind energy
Open Access WIND ENERGY SCIENCE DISCUSSIONS

Table 3. Performance overview of time domain results for above rated conditions.

	Averaged power [MW]						Efficiency [-]		
	Mechanical		Transmitted		Electrical		Power coeff	A to B	B to C
Wind farm concept	point A		point B		point C		C_P	η_{AB}	η_{BC}
NREL reference	mean	std	mean	std	mean	std	mean	mean	mean
WT1	5.28	0.22	4.99	0.21	4.41	0.18	0.249	0.944	0.885
WT2	5.27	0.23	4.97	0.22	4.40	0.19	0.284	0.944	0.885
WT3	5.28	0.22	4.99	0.21	4.42	0.18	0.251	0.944	0.885
WT4	5.28	0.23	4.98	0.22	4.41	0.19	0.244	0.944	0.885
WT5	5.27	0.23	4.98	0.22	4.41	0.19	0.277	0.944	0.885
Total	26.4		24.9		22.1	0.92	-	-	-
Hydraulic with pressure control									
WT1	5.24	0.18	-	-	-	-	0.247	-	-
WT2	5.22	0.19	-	-	-	-	0.282	-	-
WT3	5.25	0.18	-	-	-	-	0.250	-	-
WT4	5.25	0.18	-	-	-	-	0.243	-	-
WT5	5.23	0.19	-	-	-	-	0.274	-	-
Total	26.2		24.4	1.40	21.4	1.44	-	0.931	0.87

to conventional technology; for the presented operating conditions the hydraulic wind farm overall efficiency was between $0.772 - 0.810$ compared to 0.835 excluding aerodynamic performance. The most important losses in the hydraulic concept are attributed to the variable displacement pumps and friction losses in the hydraulic network. Despite having a slower response due to high water inertia, the hydraulic concept also showed higher standard deviations in the generated electrical power due to pressure transients in the hydraulic network.

5 Conclusions

The numerical model of a hydraulic wind power plant, which is used to generate electricity in a centralized manner, was presented. The model allows to capture the most relevant physics of a wind farm including transient behaviour from the hydraulic network and Pelton turbine. Despite the stochastic turbulent wind input and wake effects, the hydraulic wind farm is able to produce electricity with reasonable performance. A constant pressure controller was used in the nozzle spear valve, to avoid the excitation of flow and pressure dynamics in the hydraulic network.

The performance of the hydraulic wind farm was compared with a reference wind farm using conventional technology. For the presented case study, results indicate that the individual wind turbines are able to operate within operational limits with the current control concept. Compared to the reference wind farm, the hydraulic collection and transmission has a lower efficiency

Wind Energ. Sci. Discuss., doi:10.5194/wes-2016-54, 2016
Manuscript under review for journal Wind Energ. Sci.
Published: 20 December 2016

eawe european academy of wind energy
Open Access WIND ENERGY SCIENCE DISCUSSIONS

due to the losses induced by the variable displacement water pumps and friction losses in the hydraulic network. Further work includes the evaluation of alternative control strategies and different load cases, such as extreme wind gust, start-up and shutdown conditions, to assist the performance evaluation of the proposed centralized electricity generation approach.

Wind Energ. Sci. Discuss., doi:10.5194/wes-2016-54, 2016
Manuscript under review for journal Wind Energ. Sci.
Published: 20 December 2016

eawe european academy of wind energy
Open Access WIND ENERGY SCIENCE DISCUSSIONS

References

Buhagiar, D., Sant, T., and Bugeja, M.: A Comparison of Two Pressure Control Concepts for Hydraulic Offshore Wind Turbines, Journal of Dynamic Systems, Measurement, and Control, 2016.

Diepeveen, N.: On the Application of Fluid Power Transmission in Offshore Wind Turbines, Ph.D. thesis, Technical University of Delft, 2013.

Frandsen, S., Barthelmie, R., Pryor, S., Rathmann, O., Larsen, S., and Højstrup, J.: Analytical Modelling of Wind Speed Deficit in Large Offshore Wind Farms, Wind Energy, 9, p.39–53, 2006.

Grunnet, J., Soltani, M., Knudsen, T., Kragelund, M., and Bak, T.: Aeolus toolbox for dynamics wind farm model, simulation and control, in: The European Wind Energy Conference & Exhibition, EWEC 2010, 2010.

Jarquin Laguna, A.: Modeling and Analysis of an Offshore Wind Turbine with Fluid Power Transmission for Centralized Electricity Generation, Journal of Computational and Nonlinear Dynamics: Special issue wind turbine modelling, 10, pp.11–24, 2015.

Jarquin Laguna, A., Diepeveen, N., and Van Wingerden, J.: Analysis of dynamics of fluid power drive-trains for variable speed wind turbines: Parameter study, IET Renewable Power Generation, 8, pp.398–410, 2014.

Jensen, N.: A note on wind generator interaction, Tech. rep., Risø National Laboratory, 1983.

Jonkman, J., Butterfield, S., Musial, W., and Scott, G.: Definition of a 5MW Reference Wind Turbine for Offshore System Development, Technical report NREL/TP-500-38060, National Renewable Energy Laboratory, Golden, Colorado, 2009.

Makinen, J., Pertola, P., and Marjamaki, H.: Modeling Coupled Hydraulic-Driven Multibody Systems using Finite Element Method, in: The 1st Joint International Conference on Multibody System Dynamics, Lappeenranta University of Technology, 2010.

Merritt, H.: Hydraulic control systems, John Wiley & Sons, 1967.

Murrenhoff, H.: Systematic approach to the control of hydrostatic drives, Proceedings of the Institution of Mechanical Engineers.Part I: Journal of Systems and Control Engineering, 213, 333–347, 1999.

Thake, J.: The Micro-hydro Pelton Turbine Manual, Practical Action Publishing, 2000.

Veers, P. S.: Three-Dimensional Wind Simulation, Tech. Rep. SAND88-0152 UC-261, Sandia National Laboratories, 1988.

Zhang, Z.: Flow interactions in Pelton turbines and the hydraulic efficiency of the turbine system, Proceedings of the Institution of Mechanical Engineers, Part A: Journal of Power and Energy, 221, 343–357, 2007.